Role of the Pepino mosaic virus 3 '-untranslated region elements in negative-strand RNA synthesis in vitro

Osman, T.A.M.; Olsthoorn, R.R.C.L.; Livieratos, I.C.

Virus Research 190 (2014) 110–117

Contents lists available at ScienceDirect

Virus Research

journal homepage: www.elsevier.com/locate/virusres

Role of the *Pepino mosaic virus* 3′-untranslated region elements in negative-strand RNA synthesis *in vitro*

Toba A.M. Osman[a,b], René C.L. Olsthoorn[c,**], Ioannis C. Livieratos[a,*]

[a] Department of Sustainable Agriculture, Mediterranean Agronomic Institute of Chania, Alsylio Agrokepion, GR-73100 Chania, Crete, Greece
[b] Department of Agricultural Botany, Faculty of Agriculture, Fayoum University, Fayoum 63514, Egypt
[c] Department of Molecular Genetics, Leiden Institute of Chemistry, P.O. Box 9502, 2300 RA Leiden, The Netherlands

ARTICLE INFO

Article history:
Received 31 March 2014
Received in revised form 27 June 2014
Accepted 27 June 2014
Available online 19 July 2014

Keywords:
3′-Untranslated region
RNA replication
Potexviruses
Pepino mosaic virus
S. lycopersicum

ABSTRACT

Pepino mosaic virus (PepMV) is a mechanically-transmitted positive-strand RNA potexvirus, with a 6410 nt long single-stranded (ss) RNA genome flanked by a 5′-methylguanosine cap and a 3′ poly-A tail. Computer-assisted folding of the 64 nt long PepMV 3′-untranslated region (UTR) resulted in the prediction of three stem-loop structures (hp1, hp2, and hp3 in the 3′–5′ direction). The importance of these structures and/or sequences for promotion of negative-strand RNA synthesis and binding to the RNA dependent RNA polymerase (RdRp) was tested *in vitro* using a specific RdRp assay. Hp1, which is highly variable among different PepMV isolates, appeared dispensable for negative-strand synthesis. Hp2, which is characterized by a large U-rich loop, tolerated base-pair changes in its stem as long as they maintained the stem integrity but was very sensitive to changes in the U-rich loop. Hp3, which harbours the conserved potexvirus ACUUAA hexamer motif, was essential for template activity. Template-RNA polymerase binding competition experiments showed that the ACUUAA sequence represents a high-affinity RdRp binding element.

1. Introduction

Positive-strand RNA viruses replicate by regulated interactions between viral proteins, viral genomic RNAs, and co-opted host factors, assembled into membrane-associated multi-component replication complexes (RC) (Mine and Okuno, 2012). In the initial replication step, the viral RNA dependent RNA polymerase (RdRp) specifically recognizes and binds to unique structures and/or sequences located at the viral genomic 3′-untranslated region (UTR), which control in *cis* viral negative-strand RNA synthesis (Dreher, 1999). *Pepino mosaic virus* (PepMV) is a mechanically-transmitted, positive-stranded RNA potexvirus with flexuous, rod shaped non-enveloped virions. PepMV has over the last two decades become endemic and is now an economically-important tomato pathogen in many countries of the world (Hanssen and Thomma, 2010). Typically, PepMV possesses an approximately 6410 nt single-stranded (ss), positive-strand RNA genome with a 5′-methylguanosine cap and a 3′ poly-A tail. The coding region is flanked by the 5′- and 3′-UTRs of 86 and 64 nt in length, respectively and contains five open reading frames encoding for a 164-kDa RdRp, three triple gene block proteins (TGBp1-3) of 26, 14 and 9 kDa, and the 25-kDa coat protein (CP) (Fig. 1A; Aguilar et al., 2002). PepMV, in agreement with the prototype potexvirus, potato virus X (PVX), produces three 3′-co-terminal subgenomic (sg) RNAs expressing the TGBp1-3 and CP proteins (Verchot et al., 1998; Sempere et al., 2011; Osman et al., 2012).

For potexviruses, secondary and tertiary structures involved in negative-strand synthesis have been identified in the 3′-UTRs of bamboo mosaic virus (BaMV; Cheng and Tsai, 1999; Tsai et al., 1999) and PVX (Pillai-Nair et al., 2003). In the case of the PVX 3′-UTR, the RNA folds into three stem loops (SL1, SL2, SL3; counting from the 3′ end) (Pillai-Nair et al., 2003). The BaMV 3′-UTR folds into a cloverleaf-like structure of four hairpins (ABCD) and a pseudoknot domain (E), which includes part of the 3′-poly(A) tail (Cheng and Tsai, 1999; Tsai et al., 1999). *Cis*-acting 3′-UTR sequences essential for the initiation of negative-sense genomic RNA has also been identified (Batten et al., 2003; Park et al., 2013). A potexvirus conserved hexanucleotide (ACNUAA) in the loop of one of the 3′-terminal hairpins was initially identified in clover yellow mosaic virus (CYMV; Bancroft et al., 1991) and was later found necessary for negative-strand synthesis of CYMV (White et al., 1992), BaMV (Cheng and Tsai, 1999; Chiu et al., 2002) and PVX (Pillai-Nair

* Corresponding author. Tel.: +30 28210 35000; fax: +30 28210 35001.
** Corresponding author. Tel.: +31 71 527 4419; fax: +31 71 527 4397.
E-mail addresses: olsthoor@chem.leidenuniv.nl (R.C.L. Olsthoorn), livieratos@maich.gr, yannis.livieratos@gmail.com (I.C. Livieratos).

http://dx.doi.org/10.1016/j.virusres.2014.06.018
0168-1702/

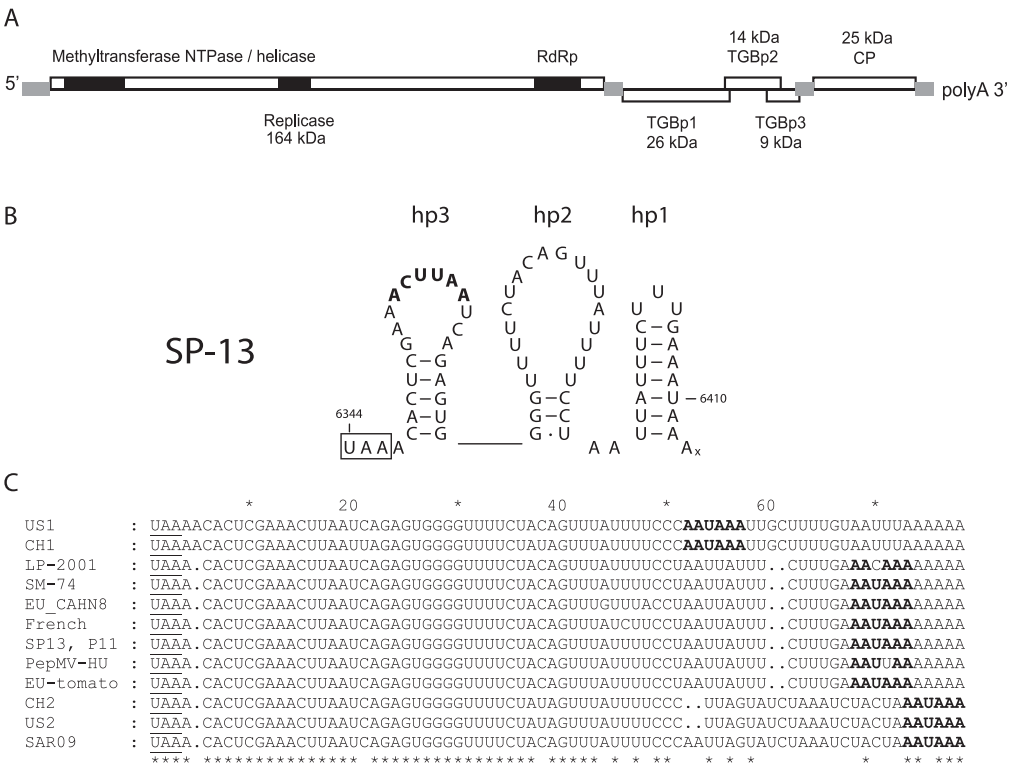

Fig. 1. Schematic representation of the PepMV genome, predicted secondary structure of the 3′-UTR and conservation of the 3′-UTR of PepMV RNA isolates. (A) Conserved protein domains in the replicase gene are indicated by black boxes. Grey boxes indicate non-coding and intergenic regions. TGB, triple gene block; CP, coat protein. (B) Predicted secondary structure of the 3′-UTR of PepMV–SP13. The termination codon of the CP gene is indicated by a rectangle. Conserved potexvirus hexamer is shown in bold face. The poly(A) tail is indicated by Ax. (C) Alignment of 3′-UTRs of PepMV isolates. The stop codon and the putative polyadenylation signal are marked. Conserved nucleotides are marked by an asterisk below the sequence. Dots were introduced to maximize the alignment. GenBank accession numbers: US1 isolate, FJ940225; SP13 isolate, NC_004067; SAR09 isolate, HQ663890; LP-2001 isolate, AJ606361; French isolate, AJ438767; EU_CAHN8 isolate, JQ314457; CH1 isolate, DQ0009840; EU-tomato isolate, FJ940223; PepMV-HU isolate, AM491606.

et al., 2003). PVX SL1 is not required for negative-strand synthesis but an eight nucleotide U-rich sequence located in SL2, which is a site of host protein binding, are essential for positive- and negative-strand synthesis (Sriskanda et al., 1996; Pillai-Nair et al., 2003). The putative adenylation signals (PAS) for BaMV and white clover mosaic potexvirus (WClMV) are also shown to be important for negative-strand synthesis and in the case of the latter, virus infectivity (Guilford et al., 1991; Chen et al., 2005). Interestingly, PVX long distance RNA–RNA interactions between 5′- and 3′-termini and subsets of identical internal octanucleotides play essential roles for both positive- and negative-strand RNA synthesis (Hu et al., 2007).

A potential problem with studies of *cis*-acting sequences in virus replication *in vivo* in plants and protoplasts is that mutations may have pleiotropic effects. One way to dissect *in vitro*, 3′-UTR RNA sequences and structures involved in negative viral RNA synthesis is *via* the isolation of transcriptionally-active, template-specific RC from infected plants (Hayes and Buck, 1990; Quadt and Jaspars, 1990; Song and Simon, 1994; Osman and Buck, 1996; Deiman et al., 1997; Singh and Dreher, 1997; Plante et al., 2000; Cheng et al., 2001; Panavas et al., 2002). We have recently developed such an *in vitro* template-dependent system, able to specifically catalyze the transcription of PepMV virion RNA, *in vitro*-synthesized full-length positive-strand RNA and 3′-terminal RNA templates of both positive- and negative-strands in the absence of protein synthesis (Osman et al., 2012). Here, we have used this system on short 3′-co-terminal PepMV RNA mutants and combined with competition assays to test the role of secondary structure elements of PepMV 3′-UTR in the initiation of negative-strand synthesis and RdRp binding.

2. Materials and methods

2.1. Plasmids, plant material and virus source

The infectious clone pTOPO-T7 PepXL6 (Sempere et al., 2011) was kindly supplied by Dr. M. Aranda (CEBAS/CSIC, Murcia, Spain). Tomato mosaic virus (ToMV)-infected tissue was kindly provided by Professor N. Katis, Aristotle University of Thessaloniki, Greece.

2.2. Prediction of the PepMV 3′-UTR structure

MFOLD was used to predict the secondary structure of the PepMV 3′-UTR (Zuker, 2003; http://mfold.rit.albany.edu/).

2.3. Synthesis of RNA templates for PepMV RdRp assays and protoplast inoculation

DNA fragments representing differently sized sequences of the PepMV positive-strand genome were PCR-amplified using the pTOPO-T7 PepXL6 DNA template and LA Taq DNA polymerase (TAKARA). All forward oligonucleotide primers contained a T7 promoter (underlined) at the 5′-end (t1, t72, t71) and were respectively designed 290, 113 and 64 nt upstream the actual 3′-end of the PepMV genome. These primers were combined with reverse primers (lacking the T7 RNA promoter) designed to confer specific mutations and target different parts of the predicted PepMV RNA secondary structures and sequences (Table 1). The PCR-generated products were purified by agarose gel electrophoresis and used as templates for *in vitro* transcription using the mMESSAGE mMACHINE T7 RNA kit (Ambion). RNA transcription products were

Table 1
List of oligonucleotide primers used in this study for RNA synthesis.

Name	Primer sequence (5′–3′)[a]	PepMV nucleotide position[b]
t5	5′-*cgaaatt*aatacgactcactatagaaaacaaaataaataaata-3′	1–20 nt
t1	5′-*cgaaatt*aatacgactcactatagcttcttcgatggagtcacca-3′	6121–6140 nt
t72	5′-gtaatacgactcactatagggaggagctaacaccatgtacgcg-3′	6298–6322 nt
t71	5′-gtaatacgactcactataggcactcgaaacttaatcagagtgggg-3′	6348–6372 nt
delhp1a	5′-ttttttttttttttttttttattaggaaaataaactgtagaaaacccc-3′	*c*6369–6399 nt-poly(A)$_{17}$
delhp1b	5′-ttttttttttttttttttttgggaaaataaactgtagaaaacccc-3′	*c*6369–6393 nt-poly(A)$_{20}$
t31	5′-ttttttttttttttttttttttttttttttttttttttttttttatttcaaaga-3′	*c*6401–6410 nt-poly(A)$_{40}$
t33	5′-ttttttttttttttttttttatttcaaaga-3′	*c*6401–6410 nt-poly(A)$_{20}$
t34	5′-ttttttttttttttatttcaaaga-3′	*c*6401–6410 nt-poly(A)$_{15}$
t2	5′-ttttttttttatttcaaagaaataa-3′	*c*6396–6410 nt-poly(A)$_{10}$
t73	5′-atttcaaagaaataatttagg-3′	*c* 6391–6410 nt
Hp2.1	5′-ttttttttttttttttttttgggaaaataaactgtagaaaaccTcactctg-3′	*c*6363–6393 nt-poly(A)$_{20}$
Hp2.2	5′-ttttttttttttttttttttAggaaaataaactgtagaaaaccTcactctg-3′	*c*6363–6393 nt-poly(A)$_{20}$
Hp2.3	5′-ttttttttttttttttttttgggTaaataaactgtagaaaacccc-3′	*c*6369–6393 nt-poly(A)$_{20}$
Hp2.4	5′-ttttttttttttttttttttgggGaaataaactgtagaaaCccccactctg-3′	*c*6363–6393 nt-poly(A)$_{20}$
Hp2.5	5′-ttttttttttttttttttttgggaaaataaactgtagaaaacGccactctg-3′	*c*6363–6393nt-poly(A)$_{20}$
Hp2.6	5′-ttttttttttttttttttttgCgaaaataaactgtagaaaacGccactctg-3′	*c*6363–6393 nt-poly(A)$_{20}$
Hp2.7	5′-ttttttttttttttttttttCCAGaaaataaactgtagaaaaCTGGcactctg-3′	*c*6363–6393 nt-poly(A)$_{20}$
Lp2.1	5′-ttttttttttttttttttttgggaaaataaactgt-gaaaaccccactctg-3′	*c*6363–6393 nt-poly(A)$_{20}$
Lp2.2	5′-ttttttttttttttttttttgggaaaataaactTtagaaaaccccactctg-3′	*c*6363–6393 nt-poly(A)$_{20}$
Lp2.3	5′-ttttttttttttttttttttgggaaaataaaTtgtagaaaaccccactctg-3′	*c*6363–6393 nt-poly(A)$_{20}$
Lp2.4	5′-ttttttttttttttttttttgggaaaataaactgtaAaaaaccccactctg-3′	*c*6363–6393 nt-poly(A)$_{20}$
Lp2.5	5′-ttttttttttttttttttttgggaaaa_aaactgtagaaaacccc-3′	*c*6369–6393 nt-poly(A)$_{20}$
Lp2.6	5′-ttttttttttttttttttttgggaaaataaactgtagaaGaccccactctg-3′	*c*6363–6393 nt-poly(A)$_{20}$
Lp2.7	5′-ttttttttttttttttttttgggaGaataaactgtagaaaacccc-3′	*c*6369–6393 nt-poly(A)$_{20}$
Hp3.1	5′-ttttttttttttttttttttgggaaaataaactgtagaaaaccccactctgattaagtttcgTCAgtttaaagttcaggg-3′	*c*6333–6393 nt-poly(A)$_{20}$
Hp3.2	5′-ttttttttttttttttttttgggaaaataaactgtagaaaaccccTGActgattaagtttcgTCAgtttaaagttcaggg-3′	*c*6333–6393 nt-poly(A)$_{20}$
Lp3.1	5′-ttttttttttttttttttttgggaaaataaactgtagaaaaccccactctgatt-tttcgagtgtttaaagttcaggg-3′	*c*6333–6393 nt-poly(A)$_{20}$
Lp3.2	5′-ttttttttttttttttttttgggaaaataaactgtagaaaaccccactctgaAATagtttcgagtgtttaaagttcaggg-3′	*c*6333–6393 nt-poly(A)$_{20}$
ToMV-17	5′-*cgaaatt*aatacgactcactataggtactggactgtacaatcag-3′	6110–6128
ToMV-18	5′-tgggccccaaccggggttc-3′	*c*6366–6384

Sequences complementary to the PepMV sequence are prefixed with a "*c*". Deletions are indicated by dashes.

[a] Mutations in the PepMV sequence are shown in bold. The T7 promoter and the polyadenylation signal sequences are underlined and grey shaded, respectively. Non-PepMV nucleotide stretches upstream the T7 promoter is shown in italics.

[b] Numbers refer to the PepMV SP13 and ToMV sequences (accession numbers 484251 and AF155507).

named after the two oligonucleotide primers used for PCR and were purified as described in the Ambion manual, assayed spectrophotometrically, and used in template-dependent RdRp assays or competition experiments.

For protoplast experimentation, full length PepMV cDNA fragments were PCR-amplified using the pTOPO-T7 PepXL6 as template, t5 forward oligonucleotide primer and a set of 3′-*co*-terminal reverse oligonucleotide primers were designed to include the polyadenylation signal and identical mutations to respective reverse primers used in the RdRp assays (Table 1). Twenty μl volume transcriptions were run as above in the presence of 2 mM m^7GpppG cap analogue. Five μg of the resulting RNA transcripts were used to PEG-inoculate protoplasts (4×10^5 cells) prepared from tomato leaves before incubation for 24 h at 25 °C under constant light. Protoplasts were harvested and total RNA was isolated with the Trizol kit according to manufacturer's instructions (Invitrogen) for subsequent Northern blot analysis using a ^{32}P-labelled probe corresponding to the 290 nt terminal fragment of the PepMV plus-strand genome as described by Osman and Buck (1996).

2.4. Template-dependent PepMV RdRp assays

The preparation of extracts containing template-dependent RdRp activity was carried out mainly as described by Osman et al. (2012) using batches (50–100 g) of PepMV-infected tomato plants harvested 5 days post inoculation. Equal amounts of each template RNA was added into the reactions, gels were dried and exposed to film and band intensities on autoradiograms were measured using a Bio-Rad Gel Documentation 144 XR System and Quantity-One software (version 4.6.5, Bio-Rad 145 Laboratories).

2.5. Competition experiments

For template competition experiments, RNA polymerase reactions were carried out as above with control RNA template t72/t31 (Table 1) at 12.5 nM and various competitor RNAs at increasing concentration. RNA template t72/t31 and competitor RNA were mixed prior to addition to the RNA polymerase reaction mixture. A ToMV 3′-UTR RNA (275 nt) template was used as a non-specific RNA competitor. The respective cDNA fragment was RT-PCR amplified from ToMV infected plants using Primescript reverse transcriptase, Pyrobest DNA polymerase (TAKARA) and primers ToMV-T17 and ToMV-T23 (Table 1). PCR-amplified product T17/T23 was used as described above to generate RNA template.

3. Results

3.1. Computer prediction of the 3′-UTR of PepMV plus-strand RNA

Structural analysis of the 3′ terminal 70 nt of the positive-strand of PepMV RNA SP-13 isolate by the MFOLD programme (Zuker, 2003) resulted in the prediction of three consecutive stem-loops (hp1, hp2, hp3, Fig. 1A and B). hp1 includes two A residues of the polyA-tail and harbours a PAS (AAUAAA). The hp2 consists of a stem of three base pairs (bps) and a loop of 18 nt. The hp3 stem is comprised of five bps and features a 12-nt loop containing the conserved potexvirus hexanucleotide ACUUAA (6355–6361 nt). Comparison with other PepMV isolates (Fig. 1C) shows that hp3 and hp2 are strongly conserved whereas hp1 is variable, although in all cases capable of forming an AU-rich hairpin. The position of the PAS motif also varies among the isolates.

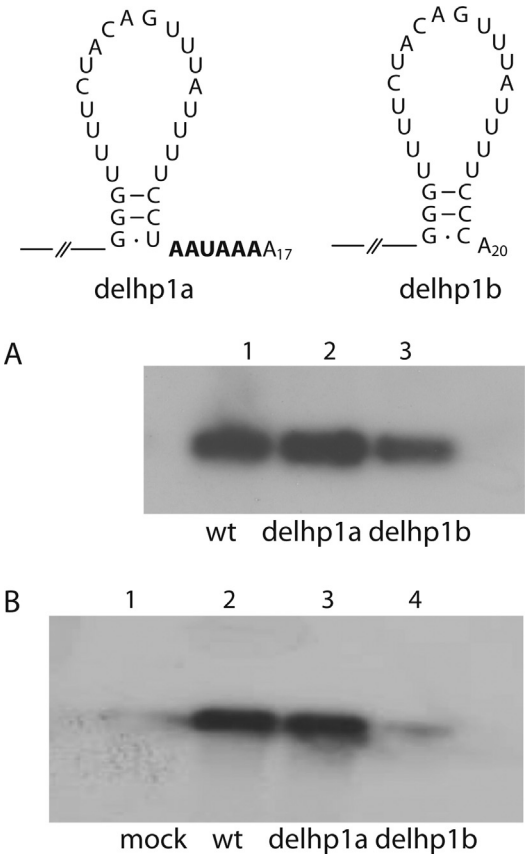

Fig. 2. Role of hp1 and polyadenylation signal in negative-strand RNA synthesis. (A) *In vitro* template-dependent RdRp assays using equally added wild-type (t1/t33) template of 290 nt (lane 1), or mutant dehlhp1a which lacks hp1 but maintains the polyadenylation signal (PAS) (lane 2), or mutant delhp1b which lacks both hp1 and PAS (lane 3). Products are radioactively labelled by incorporation of ^{32}P-UTP in the negative-strand. (B) Accumulation of PepMV negative strand RNA in protoplasts after mock inoculation (lane 1), inoculation with wild type (lane 2), delhp1a (lane 3), or delhp1b (lane 4) full-length transcripts.

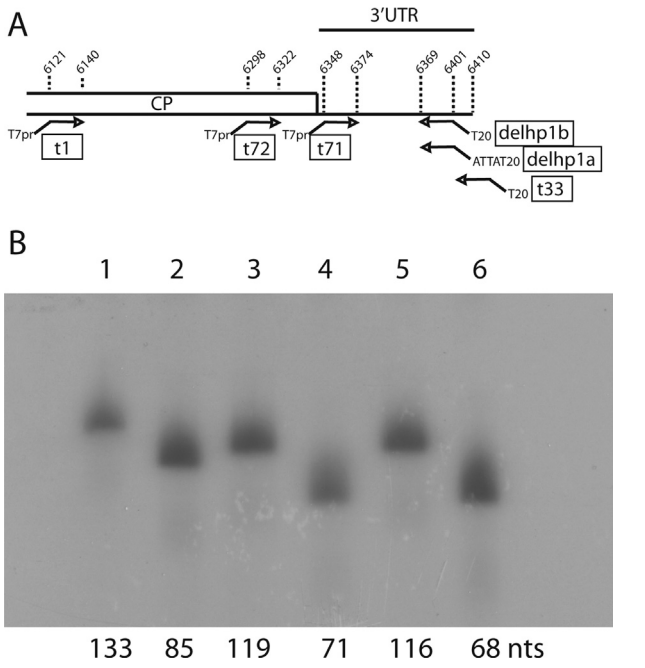

Fig. 3. Defining the minimal PepMV RNA template size for *in vitro* RdRp assays. (A) Schematic overview of primers used to generate the various templates. (B) Names and corresponding sizes (in parenthesis) of input RNA templates in lanes 1–6: t72/t33 (133 nt), t71/t33 (85 nt), t72/delhp1a (119 nt), t71/delhp1a (71 nt), t72/delhp1b (116 nt), t71/delhp1b (68 nt), respectively.

3.2. *hp1 and the polyadenylation signal are dispensable for negative-strand synthesis*

First, the importance of PepMV hp1 and PAS for negative-strand synthesis was examined in order to facilitate the design of mutant templates for downstream RdRp assays. To this end, two reverse primers were designed each to combine with the forward primer t1 (Table 1): "delhp1a" to remove hp1 but to preserve the PAS, and "delhp1b" to remove both hp1 and PAS. In the generated t1/delhp1b RNA template, the G-U bp at the bottom of hp2 was replaced by G-C to stabilize the stem as naturally occurs in US1 and other PepMV isolates (Fig. 1C). Both t1/delhp1a and t1/delhp1b RNAs served as efficient templates for PepMV RdRp (Fig. 2A) indicating that PAS and hp1 are dispensable for negative-strand synthesis.

In protoplasts however, PAS was essential for accumulation of PepMV RNA, as delhp1a but not delhp1b was able to replicate (Fig. 2B, compare lanes 3 and 4). *In vivo*, PAS is very likely required for translation of PepMV RNA in order to produce the PepMV RdRp at all. The observation that delhp1a RNA accumulated to the same level as wt PepMV RNA (Fig. 2B, compare lanes 2 and 3) indicates that hp1 is also dispensable *in vivo* for replication of PepMV (although a role in whole plants cannot be ruled out yet).

3.3. *Delineating the minimal template size for negative-strand synthesis*

In the above constructs used for RdRp *in vitro* assays, the 5′ end of the template was located 290 nt upstream of the 3′ terminus (t1 position: 6121 nt). By PCR mutagenesis, templates were truncated at the 5′ end to position 6298 and 6348 nt using forward primers t72 and t71 respectively, in combinations with reverse primers t33, delhp1a and delhp1b. The six resulting RNA templates (t72/t33, t71/t33, t72/delhp1a, t71/delhp1a, t72/delhp1b, t71/delhp1b) had 20A residues but two (116- and 68-nt long) template RNAs (t72/delhp1b and t71/delhp1b, respectively) did not carry the hp1. As can be seen in Fig. 3, all templates were active in negative-strand synthesis, with the smallest (t71/delhp1b) being the most active (taking into consideration the lower number of radioactive U's that can be incorporated). The higher activity of the t71/delhp1b RNA template may also be due to the stabilization of hp2 by the G–C bp as opposed to the G–U bp in the 71 nt construct. The t71/delhp1b RNA template served thus as the basis for downstream mutational analyses using the RdRp assays.

3.4. *hp3 stem structure and the conserved ACNUAA hexamer in loop 3 are required for negative-strand RNA synthesis*

To test the importance of the predicted hp3 stem, two drastic mutations were introduced into the central three bps of the stem; one destroying (hp3.1) and one restoring the base-pairing potential of hp3.1 (hp3.2). PepMV template-dependent RdRp could only recognize RNA mutant t71/hp3.2 suggesting the importance of structure rather than sequence of hp3 for negative-strand RNA synthesis (Fig. 4, compare lanes 2 and 3).

To examine the importance of the conserved potexvirus hexanucleotide motif (ACUUAA) in PepMV negative-strand RNA synthesis, RNA mutants t71/lp3.1 containing a 3-nt (CUU) deletion and

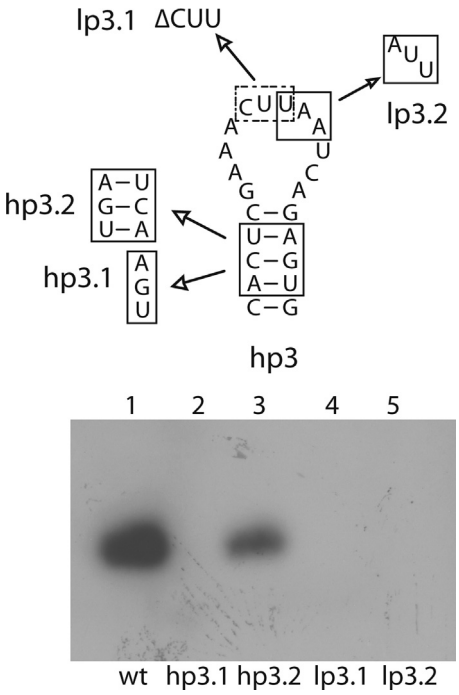

Fig. 4. Effect of hp3 mutations on negative-strand RNA synthesis *in vitro*. Lane 1, wild type (t71/t33); lane 2, hp3.1; lane 3, hp3.2; lane 4, lp3.1; lane 5, lp3.2.

t71/lp3.2, having a UAA to AUU substitution of the hexamer were used. As can be seen in Fig. 4, both mutants exhibited no detectable RdRp-template activity confirming the importance of the predicted conserved hexanucleotide sequence in the initiation of the negative-strand RNA synthesis (Fig. 4, lanes 3 and 4).

3.5. Base pairing in hp2 is essential for negative-strand synthesis

To test several aspects of the predicted hp2 structure for RNA negative-strand synthesis using the RdRp assay, specific mutants were generated following design of new oligonucleotide primers based on delph1b. Disruption of the bottom bp in hp2 by a G to A substitution, mutant hp2.1, proved lethal for replication (Fig. 5A, lane 2). The compensatory mutant hp2.2, which has an AU bp, restored negative-strand synthesis to ~30% of wt (lane 3). The lower than wt activity maybe the result of the lower thermodynamic stability of the stem in hp2.2 ($\Delta G = -4.94$ kcal/mol *vs* −6.22 for wt at 30 °C (calculated at MFOLD webserver using version 2.3 energies, which allows for adjustment of the temperature to 30 °C). Similar results were obtained by disrupting (hp2.5) and restoring (hp2.6) the middle base pair (lanes 7 and 8). In the latter case, however, the activity was restored to wt level indicating that preserving the thermodynamic stability of hp2 is important: ΔG hp2.6 −5.78 kcal/mol. Creating an additional base pair by a U to A change (hp2.3, ΔG −8.5 kcal/mol) caused a significant reduction in template activity (lane 4) whereas the presence of an G–C pair at this position (hp2.4, ΔG −9.33 kcal/mol) was detrimental for negative-strand synthesis (lane 5). Finally, replacing the entire stem by that of the corresponding stem of PVX (hp2.7, ΔG −6.94 kcal/mol) resulted in a non-active template (lane 9). Although the higher than wt stability of the latter three mutants may represent a problem for the RdRp to transcribe through (during the initiation phase), it could also be that the increased stem length or the reduced size of the U-rich loop sequences (mutated in hp2.3 and 2.4) changed the orientation of important elements for template recognition.

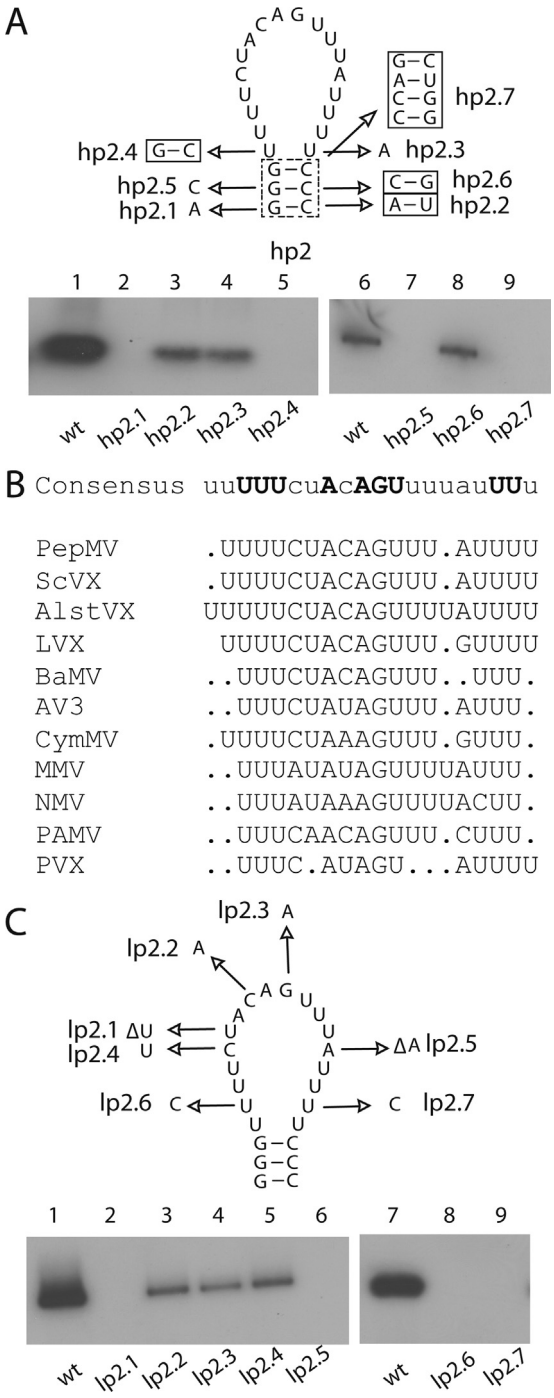

Fig. 5. (A) Effect of mutations in the PepMV hp2 stem on negative-strand RNA synthesis *in vitro*. Lane 1, wt; lane 2, hp2.1; lane 3, hp2.2; lane 4, hp2.3; lane 5, hp2.4; lane 6, wt; lane 7, hp2.5; lane 8, hp2.6; lane 9, hp2.7. (B) Comparison of the nucleotide sequences in loop 2 between several potexvirus 3′-UTRs. PepMV (GenBank accession number NC_004067); ScVX, *Scallion virus X* (NC_003400); AlstVX, *Alstroemeria virus X* (NC_007408); LVX, *Lily virus X* (NC_007192); BaMV, *Bamboo mosaic virus* (NC_001642); AV3, *Asparagus virus 3* (NC_010416); CymMV, *Cymbidium mosaic virus* (NC_001812); MMV, *Malva mosaic virus* (NC_008251); NMV; *Narcissus mosaic virus* (NC_001441); PAMV, *Potato aucuba mosaic virus* (NC_003632); PVX, *Potato virus X* (NC_011620). (C) Effect of mutations in the PepMV hp2 loop (lp) on negative-strand RNA synthesis *in vitro*. Lane 1, wt (t71/delphb); lane 2, lp2.1; lane 3, lp2.2; lane 4, lp2.3; lane 5, lp2.4; lane 6, lp2.5; lane 7, wt; lane 8, lp2.6; lane 9, lp2.7.

3.6. Effects of hp2 loop point mutations on negative-strand RNA synthesis

Comparison of the loop 2 sequences between several potexvirus RNAs revealed a high degree of conservation (Fig. 5B). Based on this alignment, we chose to mutate five positions in loop 2 of PepMV (Fig. 5C): lp2.1, deletion of U, increasing the resemblance to PVX; lp2.2, C to A change as in Cymbidium mosaic virus and Narcissus mosaic virus; lp2.3, change of the highly conserved G to A; lp2.4, increasing length of the 5′ U-stretch by C to U change; lp2.5, increasing the length of the 3′ U-stretch by deletion of A8386. In the RdRp assay, both deletion mutations lp2.1 and lp2.5 completely lost their template activity (Fig. 5C, lanes 2 and 6). The other three mutants were approximately 3 to 4-fold less active than wild type (wt) RNA template (t71/delhp1. In addition, two single C to U mutants in the highly conserved U-rich sequences on either side of the loop (lp2.6 and lp2.7) were tested and found to be inactive (Fig. 5C).

3.7. Competition assays

Competition analysis with different regions of the BaMV 3′-UTR showed that an *Escherichia coli*-expressed RdRp domain binds to at least two independent RNA binding sites, the potexviral conserved hexamer motif at stem-loop D and the poly(A) tail (Huang et al., 2001). For PepMV, an RNA template competition assay was performed to investigate the ability of certain inactive mutant PepMV RNAs to compete with the wt RNA (t72/t31) carrying a poly(A) tail of 40 residues, which previously was shown to represent a highly effective RNA template (Osman et al., 2012). This would separate the requirement of the RdRp to bind to specific RNA sites from the ability of RNA mutants to serve as templates for negative-strand synthesis. Initially, as a positive control to test the efficacy of the competition assay, a 93-nt long RNA carrying 20 residues at its poly(A) tail (t71/t33), which could act as a template (Fig. 1) and readily be separated by PAGE from the t72/t31 transcript (generating a 153-nt product followed by a poly(A) tail of 40 A residues) was tested for its ability to inhibit synthesis of the latter. As expected, t71/t33 could efficiently compete with t72/t31 RNA template at molar levels of 10, 20, 40 and 75 nM (Fig. 6A). RNA t71/t33 acted as an efficient competitor and also as a template for the PepMV RdRp. It was therefore of interest to determine if PepMV RNAs with mutations in the 3′-UTR, which do not act as templates for the RdRp, can competitively bind to the RdRp. RNA templates t71/lp2.1 and t71/lp3.1, were tested for their ability to compete with the t72/t31 template in RdRp assays and the former carrying a single U deletion in the hp2 loop could efficiently compete at molar amounts above 40 nM. In contrast, template t71/lp3.1, which carries a 3 nt deletion in the potexvirus hexamer, was not a competitor for RdRp binding at all concentrations (10–100 nM) as it did not adversely affect the amount of t72/t31 RNA synthesis indicating that the mutated lp3.1 sequence, or any of the multiple internal sequences, did not compete significantly for RdRp binding. An RNA corresponding to the 3′-terminal 275 nt of ToMV RNA was a poor competitor, having only a slight effect on negative-strand RNA synthesis directed by PepMV template t72/t31 at concentrations up to 100 nM (Fig. 6B) showing that ToMV RNA carries no binding sites for the PepMV RdRp.

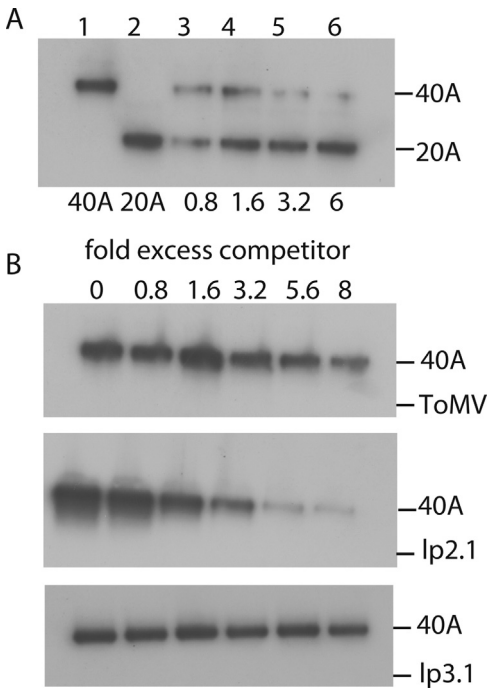

Fig. 6. Competition assays between template t72/t31 (40A) and several others for binding to the PepMV RdRp. (A) Competition between a short t71/t33 (20A) and long t72/t31 (40A) wt template. t72/t31 (40A) concentration was kept at 12.5 nM while t71/t33 (20A) was used at various concentrations. Lane 1, t72/t31 alone (12.5 nM); lane 2, t71/t33 alone (12.5 nM); lane 3, t71/t33 (10 nM); lane 4, t71/t33 (20 nM); lane 5, t71/t33 (40 nM); lane 6, t71/t33 (75 nM). (B) t72/t31 (40A) concentration was kept at 12.5 nM concentration while ToMV (T17/T18), t71/lp2.1 and t71/lp3.1 were present at 0 nM (lane 1), 10 nM (lane 2), 20 nM (lane 3), 40 nM (lane 4), 70 nM (lane 5) and 100 nM (lane 6). The migration of the expected products is indicated on the right side of the gels.

4. Discussion

Secondary and tertiary structures and sequences of the 3′ UTR of potexviruses have been identified as well as a number of their function(s) (Tsai et al., 1999; Cheng and Tsai, 1999; Pillai-Nair et al., 2003). For the PepMV 3′ UTR, the proposed two-dimensional structure was tested experimentally here in negative-strand RNA synthesis using RdRp assays. Similarly to PVX (Pillai-Nair et al., 2003), PepMV RNA transcripts lacking hp1 (delhp1a and delhp1b) could also promote negative-strand RNA synthesis with similar efficiency to the wt RNA (Fig. 2A) and the absence of a polyadenylation signal (PAS) had no effect on negative-strand synthesis. Previously, it was shown that the PAS motif is involved in BaMV negative-strand RNA synthesis in protoplasts (Chen et al., 2005). However, it could not be ruled out that this motif was required for polyadenylation and/or translation of BaMV RNAs.

The data from mutational analysis of PepMV hp2 and hp3, clearly demonstrated a requirement for these stem structures for negative-strand RNA synthesis. Firstly, our data confirmed the importance of the potexvirus conserved hexamer motif for negative-strand synthesis initiation as demonstrated for WClMV (White et al., 1992), BaMV (Cheng and Tsai, 1999; Chiu et al., 2002) and PVX (Pillai-Nair et al., 2003). However, for WClMV and BaMV the role of this motif in *in vitro* RdRP assays has not been tested although BaMV RdRp was found to protect it from chemical modification in a foot-printing analysis (Huang et al., 2001). Here, the deletion or disruption of the hexamer sequence motif ACUUAA residing in the hp3 loop resulted in the abolishment of negative-strand RNA synthesis (Fig. 4) and also abolished RdRp binding as indicated by the competition assays (Fig. 6). In contrast to PVX however, no upstream complementary sequences are required for optimal negative-strand synthesis by PepMV RdRp. PepMV transcripts as short as 68 nt are sufficient for negative-strand synthesis, while in the case of PVX at least 850 nt were shown to be required for efficient negative-strand synthesis. Similar octamers are present in the sgRNA promoter regions of PepMV and BaMV (data not shown) but are apparently not involved in negative-strand synthesis *in vitro*. It is also difficult to envisage how such an interaction would increase template activity, when

the motif itself in single-stranded conformation represents a high-affinity binding site for the RdRp as shown here for PepMV and previously for BaMV.

Mutations in the hp2 loop also affected negative-strand RNA synthesis (Fig. 5). It is not clear what the function of these nts is; the competition assay with lp2.1 indicated that this nt is not a determinant for RdRp binding (Fig. 6). Possibly, mutations in loop 2 change the 3D structure of the template thereby preventing initiation of negative-strand synthesis. Similar effects have been reported for TMV (Osman et al., 2000) and alfalfa mosaic virus (Olsthoorn and Bol, 2002), where mutations outside the major RdRp binding elements were suggested to affect the orientation of these elements with respect to the transcription-initiation site. The possibility that nucleotides in loop 2 are involved in some kind of 3D structure resembling *e.g.* the BaMV PK remains the subject of our future experiments.

It cannot be completely ruled out that the observed differences in template activities may represent differences in RNA stabilities, however, in the case of mutants that do not disrupt any secondary structure but even stabilize it, *e.g.* hp2.3, hp2.4, and hp2.7, it is hard to imagine that their lower template activity is caused by enhanced degradation of the template. In addition, some inactive templates, like lp2.1, are still good competitors, a finding that is also difficult to reconcile with lowered template stability.

In the RC, host factors may also physically interact with viral RNA *cis*-acting elements and in some cases are required for efficient virus replication (Zeenko et al., 2002; Isken et al., 2007; Galao et al., 2010; Li and Nagy, 2011). For BaMV, a heat shock protein 90 homologue of *Nicotiana benthamiana* has been recently reported to specifically interact with the 3′-UTR genomic RNA (Huang et al., 2012), the glycolytic enzyme glyceraldehyde 3-phosphate dehydrogenase is part of the RC and inhibits RNA synthesis (Prasanth et al., 2011) and two chloroplast phosphoglycerate kinases and p51 bind to the viral 3′-UTR also affecting RNA accumulation (Lin et al., 2007). On the same note for PVX, the replication-essential U-rich octanucleotide in hp2 is required for host protein binding (Sriskanda et al., 1996). U-rich sequences are conserved in the loop of hp2 PepMV and other potexviruses (Fig. 6) and interestingly, several of these U-rich sequences resemble the UUUUAU motif involved in cytoplasmic polyadenylation of mRNAs with short poly(A) tails ($\leq$12 nt) during *Xenopus oocyte* maturation (Fox et al., 1989; McGrew et al., 1989). It may well be that a plant cytoplasmic poly(A)-polymerase is involved in the polyadenylation of potexvirus RNAs.

Acknowledgments

We thank Dr. M. Aranda and Dr. R. Sempere for providing the PepMV cDNA infectious clone and inoculum. This work was funded by the Marie Curie IIF "Pep-Rep-2" project grant PIIF-GA-2009-235563.

References

Aguilar, J.M., Hernandez-Gallardo, M.D., Cenis, J.L., Lacasa, A., Aranda, M.A., 2002. Complete sequence of the *Pepino mosaic virus* RNA genome. Arch. Virol. 147, 2009–2015.

Bancroft, J.B., Rouleau, M., Johnston, R., Prins, L., Mackie, G.A., 1991. The entire nucleotide-sequence of *Foxtail mosaic virus* RNA. J. Gen. Virol. 72, 2173–2181.

Batten, J.S., Yoshinari, S., Hemenway, C., 2003. Potato virus X: a model system for virus replication, movement and gene expression. Mol. Plant Pathol. 4, 125–131.

Chen, I.H., Chou, W., Lee, P.Y., Hsu, Y.H., Tsai, C.H., 2005. The AAUAAA motif of *Bamboo mosaic virus* RNA is involved in minus-strand RNA synthesis and plus-strand RNA polyadenylation. J. Virol. 79, 14555–14561.

Cheng, C.P., Tsai, C.H., 1999. Structural and functional analysis of the 3′-untranslated region of bamboo mosaic potexvirus genomic RNA. J. Mol. Biol. 288, 555–565.

Cheng, J.H., Ding, M.P., Hsu, Y.H., Tsai, C.H., 2001. The partial purified RNA-dependent RNA polymerases from *Bamboo mosaic potexvirus* and *Potato virus* X infected plants containing the template-dependent activities. Virus Res. 80, 41–52.

Chiu, W.W., Hsu, Y.H., Tsai, C.H., 2002. Specificity analysis of the conserved hexanucleotides for the replication of bamboo mosaic potexvirus RNA. Virus Res. 83, 159–167.

Deiman, B.A.L.M., Seron, K., Jaspars, E.M.J., Pleij, C.W.J., 1997. Efficient transcription of the tRNA-like structure of *Turnip yellow mosaic virus* by a template-dependent and specific viral RNA polymerase obtained by a new procedure. J. Virol. Methods 64, 181–195.

Dreher, T.W., 1999. Functions of the 3′-untranslated regions of positive strand RNA viral genomes. Annu. Rev. Phytopathol. 37, 151–174.

Fox, C.A., Sheets, M.D., Wickens, M.P., 1989. Poly(A) addition during maturation of frog oocytes: distinct nuclear and cytoplasmic activities and regulation by the sequence UUUUUAU. Genes Dev. 3, 2151–2162.

Galao, R.P., Chari, A., Alves-Rodrigues, I., Lobao, D., Mas, A., Kambach, C., Fischer, U., Diez, J., 2010. LSm1-7 complexes bind to specific sites in viral RNA genomes and regulate their translation and replication. RNA 16, 817–827.

Guilford, P.J., Beck, D.L., Forster, R.L.S., 1991. Influence of the poly(a) tail and putative polyadenylation signal on the infectivity of *White clover mosaic potexvirus*. Virology 182, 61–67.

Hanssen, I.M., Thomma, B.P.H.J., 2010. Pepino mosaic virus: a successful pathogen that rapidly evolved from emerging to endemic in tomato crops. Mol. Plant Pathol. 11, 179–189.

Hayes, R.J., Buck, K.W., 1990. Complete replication of a eukaryotic virus RNA *in vitro* by a purified RNA-dependent RNA polymerase. Cell 63, 363–368.

Hu, B., Pillai-Nair, N., Hemenway, C., 2007. Long-distance RNA-RNA interactions between terminal elements and the same subset of internal elements on the *Potato virus X* genome mediate minus- and plus-strand RNA synthesis. RNA 13, 267–280.

Huang, C.Y., Huang, Y.L., Meng, M., Hsu, Y.H., Tsai, C.H., 2001. Sequences at the 3′-untranslated region of bamboo mosaic potexvirus RNA interact with the viral RNA-dependent RNA polymerase. J. Virol. 75, 2818–2824.

Huang, Y.W., Hu, C.C., Liou, M.R., Chang, B.Y., Tsai, C.H., Meng, M.H., Lin, N.S., Hsu, Y.H., 2012. Hsp90 interacts specifically with viral RNA and differentially regulates replication initiation of Bamboo mosaic virus and associated satellite RNA. PLos Pathog. 8 (5), Article Number: e1002726.

Isken, O., Baroth, M., Grassmann, C.W., Weinlich, S., Ostareck, D.H., Ostareck-Lederer, A., Behrens, S.E., 2007. Nuclear factors are involved in hepatitis C virus RNA replication. RNA 13, 1675–1692.

Li, Z., Nagy, P.D., 2011. Diverse roles of host RNA-binding proteins in RNA virus replication. RNA Biol. 8, 305–315.

Lin, J.W., Ding, M.P., Hsu, Y.H., Tsai, C.H., 2007. Chloroplast phosphoglycerate kinase, a gluconeogenetic enzyme, is required for efficient accumulation of *Bamboo mosaic virus*. Nucl. Acids Res. 35, 424–432.

McGrew, L.L., Dworkin-Rastl, E., Dworkin, M.B., Richter, J.D., 1989. Poly (A) elongation during *Xenopus* oocyte maturation is required for translational recruitment and is mediated by a short sequence element. Genes Dev. 3, 803.

Mine, A., Okuno, T., 2012. Composition of plant virus RNA replicase complexes. Curr. Opin. Virol. 2, 669–675.

Quadt, R., Jaspars, E.M., 1990. Purification and characterization of *Brome mosaic virus* RNA-dependent RNA polymerase. Virology 178, 189–194.

Olsthoorn, R.C., Bol, J.F., 2002. Role of an essential triloop hairpin and flanking structures in the 3′-untranslated region of *Alfalfa mosaic virus* RNA in *in vitro* transcription. J. Virol. 76, 8747–8756.

Osman, T.A., Buck, K.W., 1996. Complete replication *in vitro* of *Tobacco mosaic virus* RNA by a template-dependent, membrane-bound RNA polymerase. J. Virol. 70, 6227–6234.

Osman, T.A., Hemenway, C.L., Buck, K.W., 2000. Role of the 3′tRNA-like structure in *Tobacco mosaic virus* minus-strand RNA synthesis by the viral RNA-dependent RNA polymerase *in vitro*. J. Virol. 74, 11671–11680.

Osman, T.A.M., Olsthoorn, R.C.L., Livieratos, I.C., 2012. In vitro template-dependent synthesis of *Pepino mosaic virus* positive- and negative-strand RNA by its RNA-dependent RNA polymerase. Virus Res. 167, 267–272.

Panavas, T., Pogany, J., Nagy, P.D., 2002. Analysis of minimal promoter sequences for plus-strand synthesis by the *Cucumber necrosis virus* RNA-dependent RNA polymerase. Virology 296, 263–274.

Park, M.R., Seo, J.K., Kim, K.H., 2013. Viral and non-viral elements in potexvirus replication and movement and in antiviral responses. Adv. Virus Res. 87, 75–112.

Pillai-Nair, N., Kim, K.H., Hemenway, C., 2003. Cis-acting regulatory elements in the *Potato virus* X 3′-non-translated region differentially affect minus-strand and plus-strand RNA accumulation. J. Mol. Biol. 326, 701–720.

Plante, C.A., Kim, K.H., Pillai-Nair, N., Osman, T.A., Buck, K.W., Hemenway, C.L., 2000. Soluble, template-dependent extracts from *Nicotiana benthamiana* plants infected with *Potato virus X* transcribe both plus- and minus-strand RNA templates. Virology 275, 444–451.

Prasanth, K.R., Huang, Y.W., Liou, M.R., Wang, R.Y.L., Hu, C.C., Tsai, C.H., Meng, M.H., Lin, N.S., Hsu, Y.H., 2011. Glyceraldehyde 3′-phosphate dehydrogenase negatively regulates the replication of *Bamboo mosaic virus* and its associated satellite RNA. J. Virol. 85, 8829–8840.

Sempere, R.N., Gómez, P., Truniger, V., Aranda, M.A., 2011. Development of expression vectors based on *Pepino mosaic virus*. Plant Methods 7, 6.

Singh, R.N., Dreher, T.W., 1997. Turnip yellow mosaic virus RNA dependent RNA polymerase: initiation of minus strand synthesis *in vitro*. Virology 233, 430–439.

Sriskanda, V.S., Pruss, G., Ge, X., Vance, V.B., 1996. An eight-nucleotide sequence in the *Potato virus X* 3′-untranslated region is required for both host protein binding and viral multiplication. J. Gen. Virol. 70, 5266–5271.

Song, C., Simon, A.E., 1994. RNA-dependent RNA polymerase from plants infected with *Turnip crinkle virus* can transcribe (+) and (−) strands of virus-associated RNAs. Proc. Natl. Acad. Sci. U. S. A. 91, 8792–8796.

Tsai, C.H., Cheng, C.P., Peng, C.W., Lin, B.Y., Lin, N.S., Hsu, Y.H., 1999. Sufficient length of a poly(A) tail for the formation of a potential pseudoknot is required for efficient replication of bamboo mosaic potexvirus RNA. J. Virol. 73, 2703–2709.

Verchot, J., Angell, S.M., Baulcombe, D.C., 1998. In vivo translation of the triple gene block of *Potato virus* X requires two subgenomic mRNAs. J. Virol. 72, 8316–8320.

White, K.A., Bancroft, J.B., Mackie, G.A., 1992. Mutagenesis of a hexanucleotide sequence conserved in potexvirus RNAs. Virology 189, 817–820.

Zeenko, V.V., Ryabova, L.A., Spirin, A.S., Rothnie, H.M., Hess, D., Browning, K.S., 2002. Eukaryotic elongation factor 1A interacts with the upstream pseudoknot domain in the 3′-untranslated region of *Tobacco mosaic virus* RNA. J. Virol. 76, 5678–5691.

Zuker, M., 2003. Mfold web server for nucleic acid folding and hybridization prediction. Nucl. Acids Res. 31, 3406–3415.